The Journal of Immunology

Carbon Nanoparticles Inhibit the Antimicrobial Activities of the Human Cathelicidin LL-37 through Structural Alteration

Fern Findlay, Jan Pohl, Pavel Svoboda, Priyanka Shakamuri, Kevin McLean, Neil F. Inglis, Lorna Proudfoot and Peter G. Barlow

J Immunol published online 16 August 2017
http://www.jimmunol.org/content/early/2017/08/16/jimmunol.1700706

The Journal of Immunology is published twice each month by
The American Association of Immunologists, Inc.,
1451 Rockville Pike, Suite 650, Rockville, MD 20852

Print ISSN: 0022-1767 Online ISSN: 1550-6606.

Published August 16, 2017, doi:10.4049/jimmunol.1700706

Carbon Nanoparticles Inhibit the Antimicrobial Activities of the Human Cathelicidin LL-37 through Structural Alteration

Fern Findlay,* Jan Pohl,† Pavel Svoboda,† Priyanka Shakamuri,† Kevin McLean,‡ Neil F. Inglis,‡ Lorna Proudfoot,* and Peter G. Barlow*

Host defense peptides, also known as antimicrobial peptides, are key elements of innate host defense. One host defense peptide with well-characterized antimicrobial activity is the human cathelicidin, LL-37. LL-37 has been shown to be upregulated at sites of infection and inflammation and is regarded as one of the primary innate defense molecules against bacterial and viral infection. Human exposure to combustion-derived or engineered nanoparticles is of increasing concern, and the implications of nanomaterial exposure on the human immune response is poorly understood. However, it is widely acknowledged that nanoparticles can interact strongly with several immune proteins of biological significance, with these interactions resulting in structural and functional changes of the proteins involved. This study investigated whether the potent antibacterial and antiviral functions of LL-37 were inhibited by exposure to, and interaction with, carbon nanoparticles, together with characterizing the nature of the interaction. LL-37 was exposed to carbon black nanoparticles in vitro, and the antibacterial and antiviral functions of the peptide were subsequently assessed. We demonstrate a substantial loss of antimicrobial function when the peptide was exposed to low concentrations of nanomaterials, and we further show that the nanomaterial-peptide interaction resulted in a significant change in the structure of the peptide. The human health implications of these findings are significant, as, to our knowledge, this is the first evidence that nanoparticles can alter host defense peptide structure and function, indicating a new role for nanoparticle exposure in increased disease susceptibility. ***The Journal of Immunology*****, 2017, 199: 000–000.**

In globally recognized areas of high particulate air pollution, individuals are exposed to billions of nanoparticles each day, via inhalation and skin contact (1). Furthermore, many consumer products and medical applications are now using engineered nanoparticles to enhance their efficacy. Humans are therefore becoming rapidly and increasingly exposed to these particles to a greater extent than ever before (2).

The effectiveness of host defense molecules in the human innate immune system involves a complex network of structures and processes, primarily designed to protect an individual from disease through the prevention of pathogenic microbial colonization and infection. However, within the context of increased environmental concentrations of nanoparticles, the implications of nanoparticle exposure on host defense are poorly understood. It is recognized that the size of a nanoparticle can strongly affect its physicochemical properties and functionality, as well as biodistribution in an organism following exposure. It has also been demonstrated that nanoparticles can evade physical clearance mechanisms in humans, and enter or diffuse through cell membranes, leading to increased biodistribution and longer persistence in the body. In addition, it has been suggested repeatedly that the nanoparticle component of air pollution, such as particulate matter (PM_{10}), could be responsible for the increased susceptibility of individuals to respiratory infections in areas of high concentrations of air pollution by impacting the host response to the infection (3, 4). However, no firm mechanistic understanding of this link has yet been demonstrated.

Host defense peptides (HDP; also known as antimicrobial peptides) are a major component of the innate immune system. Two major families have been characterized in humans, defensins and cathelicidins, and peptides from both families have been demonstrated to possess potent immunomodulatory and antimicrobial activities (reviewed in Refs. 5–7). These peptides are regarded as key elements of the innate immune system. The sole human cathelicidin, LL-37, is the active fragment of the inactive proprotein hCAP-18, and has been shown to have potent antimicrobial and immunomodulatory activity (reviewed in Refs. 6, 8). LL-37 is generated after hCAP-18 is released from neutrophil-specific granules, and cleaved by extracellular proteinase-3 (9). The active LL-37 peptide contains 37 aa and the sequence begins at the cleavage site with two leucine residues. Although LL-37 is primarily contained within the specific granules of neutrophils, it has also been found at lower concentrations in other cells and tissues throughout the body, such as epithelial cells, monocytes, NK cells, B cells, trophoblasts, and keratinocytes (10, 11). LL-37 is normally present as a defense mechanism in saliva, tears, and other bodily fluids, and is generally upregulated during infections and inflammation. LL-37 has many immunomodulatory functions reported within the innate immune system including, but not limited to, the recruitment of inflammatory cells to a site of infection; wound healing (angiogenesis); acting as a chemotactic agent for neutrophils, monocytes, and T cells; differentiation and

*School of Applied Sciences, Edinburgh Napier University, Edinburgh EH11 4BN, United Kingdom; †Biotechnology Core Facility Branch, Centers for Disease Control and Prevention, Atlanta, GA 30333; and ‡Moredun Proteomics Facility, Moredun Research Institute, Penicuik EH26 0PZ, United Kingdom

ORCIDs: 0000-0002-4042-8058 (L.P.); 0000-0002-6516-9312 (P.G.B.).

Received for publication May 12, 2017. Accepted for publication July 22, 2017.

This work was supported by an Edinburgh Napier University Research Studentship (to F.F.) and Tenovus Scotland (E12/01) (to P.G.B.).

Address correspondence and reprint requests to Dr. Peter G. Barlow, Sighthill Campus, Edinburgh Napier University, Edinburgh EH11 4BN, U.K. E-mail address: p.barlow@napier.ac.uk

Abbreviations used in this article: ddH_2O, double distilled water; DLS, dynamic light scattering; EGS, ethylene glycolbis(succinimidylsuccinate); HDP, host defense peptide; LB, Luria–Bertani; NEAA, nonessential amino acid.

maturation of dendritic cells; regulation of cell death pathways; and broad-spectrum antimicrobial activity (6, 12–16).

It has been documented that proteins and peptides binding or interacting with nanomaterials can undergo significant structural changes, which have subsequently caused a change in function (17). Proteins contained within a biological fluid such as pulmonary surfactant can become bound to nanoparticles, and this phenomenon is termed the formation of a protein corona (18). The protein corona of a particle depends on the kinetics and binding affinities of the proteins in the surrounding fluid, and can change over time until equilibrium has been reached. As the protein concentration of biological fluids can be as much as 35% by volume, the likelihood of nanoparticles coming into contact and interacting with proteins is relatively high. However, predicting the outcome of a nanomaterial and protein interaction is difficult, as there are a number of properties of the particle, and indeed the protein, that require consideration.

In this study, we examine interactions that can occur between carbon nanoparticles and the human HDP LL-37, assessing structural and functional changes as a consequence of particle exposure. This study has significant implications for human health within the context of particulate air pollution, linking increased susceptibility to infection and nanoparticle exposure.

Materials and Methods

Reagents and materials

Gradient Tris-Glycine-HCL gels (4–20%) were purchased from Thermo Scientific, Pierce, IL. Acetic acid, isopropanol, Coomassie Blue, and Luria–Bertani (LB) agar were purchased from Sigma-Aldrich, Dorset, U.K. Human LL-37 ELISA kit (HK321) was purchased from Hycult Biotech, Plymouth Meeting, PA. Ethylene glycolbis(succinimidylsuccinate) (EGS) was purchased from Thermo Fisher Scientific, and the solutions were prepared by dissolving the weighed solid in DMSO (Sigma-Aldrich) to a final percentage of 10%. High-glucose DMEM was purchased from PAA, Pasching, Austria.

Peptides

The peptides were assembled using the Fmoc/tBu solid-phase peptide synthesis approach using either model 433A (Applied Biosystems, Foster City, CA) or model Liberty (CEM, Matthews, NC) automated peptide synthesizers followed by cleavage in the trifluoroacetic acid/phenol/thioanisole/ethanedithiol/water (10:0.75:0.5:0.25:0.5, w/w) mixture at 25˚C for 90 min, followed by precipitation with cold diethyl ether. The crude peptides were purified by preparative reversed-phase high-pressure liquid chromatography. The peptide purity (>98%) was confirmed by analytical reversed-phase high-pressure liquid chromatography, and the masses were confirmed by mass spectrometry. Following lyophilization, the purified peptides were obtained in the form of their trifluoroacetic acid salts, namely: LL-37 (LLGDFFRKSKEKIGKEFKRIVQRIKDFLRNLVPRTES), LL-37 analog having scrambled sequence (RSLEGTDRFPFVRLKNSRKLEFKDIKGIKREQFVKIL), termed sLL-37 (control peptide). All peptides were dissolved in endotoxin-free ultrapure water (Sigma-Aldrich) and stored at −20˚C until use. The lyophilized peptide (>99% purity) was resuspended in ultrapure water (5 mg/ml) (Invitrogen, Paisley, U.K.) and was stored at −20˚C.

Nanoparticle preparation

Carbon black nanoparticles (14 nm primary particle diameter, 254 m^2 per g) (Printex 90; Degussa, Germany) were suspended in ultrapure water (5 mg/ml stock solution). The stock solution was sonicated for 10 min to allow for dispersal of the particles and working solutions were vortexed for 5 s prior to dilution.

Virus propagation

Rhinovirus (RV1B) and a live culture of WI-38 fetal lung epithelial cells were purchased from Public Health England Culture Collections, Porton Down, U.K. Cells were maintained in Eagle's MEM supplemented with 10% FCS (Sigma), 1% penicillin streptomycin, 1% L-glutamine, and 1% nonessential amino acids (NEAA) (all purchased from PAA). The virus was propagated in WI-38 cells (100 μl of virus in 10 ml of infection media containing 1% penicillin streptomycin, 1% L-glutamine, and 1% NEAA, in a 75 cm^2 flask). The infected cells were then incubated for 3 h at 33˚C, 5% CO_2 to allow the virus to infect cells. The infection media was then removed by aspiration and replaced with maintenance media (containing 2.5% FCS, 1% penicillin streptomycin, 1% L-glutamine, and 1% NEAA) to maintain the cells during the propagation process. The virus was harvested 4–6 d postinfection of the cells and subjected to a freeze-thaw cycle before the medium was decanted into a centrifuge tube and centrifuged at 13,000 × *g* using a Hettich Universal 320R centrifuge (DJB Labcare, Buckinghamshire, U.K.) for 5 min. The cell pellet was discarded and viral supernatant was aliquoted into 1 ml sterile Eppendorf tubes and stored at −20˚C until required.

Bacterial strains

Cultures of *Staphylococcus aureus* (NCIB 6571; Oxford Strain), *Escherichia coli* (NCIB 86), and *Pseudomonas aeruginosa* (PAO1) (supplied by Dr. D. Fraser-Pitt, Edinburgh Napier University) were all grown in LB broth (Thermo Fisher, Loughborough, U.K.).

SDS-PAGE assessment of peptide cross-linking

LL-37 (125 μg/ml) was preincubated with carbon black nanoparticles (100 μg/ml) for 1 h at 37˚C prior to the addition of EGS (to give final concentrations of 2 and 5 mM). The EGS was incubated with the samples for 30 min, 1, and 2 h at 37˚C to assess the optimum incubation period for the cross-linking reaction to occur. EGS is known to become unstable after prolonged periods of time and therefore additional EGS was added to the samples undertaking a 2 h cross-linking reaction after 1 h. Ultrapure ddH_2O was added to the samples not containing EGS to ensure the volumes were consistent in all cases and thus all concentrations indicated are final. Gel electrophoresis was performed at 150 mV 100 mA and 30 W for 45–60 min using a Bio-Rad power pack. Gels were then placed in an isopropanol fixing solution (10% [v/v] acetic acid, 25% [v/v] isopropanol, and 65% [v/v] double distilled water [ddH_2O]), for 20–30 min and then stained using Coomassie blue stain (10% [v/v] acetic acid, 0.006% Coomassie Blue, and 90% [v/v] ddH_2O) for 1 h. Following this process, gels were destained for 1 h in 10% acetic acid and subsequently washed and left in ddH_2O. The gels were imaged using a ChemiDoc XRS+ System (Bio-Rad). Cross-linking of peptide was assessed by the presence of higher m.w. bands appearing in the presence of EGS.

ELISA

Samples were prepared with LL-37 at a concentration of 50 μg/ml and carbon black nanoparticles at varying concentrations (0, 25, 50, and 100 μg/ml). Samples were incubated at 37˚C for 4 h. An ELISA for the detection of LL-37 was performed as directed by the manufacturer's protocol. Briefly, 100 μl of each standard and sample was transferred to the appropriate well in duplicate; the plate was covered and incubated for 1 h at room temperature. The plate was then washed four times with wash buffer, diluted tracer (100 μl) was added to each well, and the plate incubated for 1 h at room temperature. The plate was washed four times with wash buffer and diluted streptavidin-peroxidase (100 μl) was added to each well. The plate was then incubated for 1 h at room temperature, then washed four times and tetramethylbenzidine substrate (100 μl) was added to each well. The plate was incubated for a further 20 min at room temperature, then stop solution (100 μl) was added to each well, and the plate was read using a Dynatech Laboratories MRX Microplate Reader at 450 nm. Sample preparation and the ELISA procedure was repeated three independent times in triplicate ($n = 3$).

MALDI-TOF mass spectrometry

MALDI-TOF mass spectrometry was performed on samples containing LL-37 alone and LL-37 exposed to carbon black nanoparticles (final peptide concentration 125 μg/ml, final particle concentration 100 μg/ml) for 4 h at 37˚C. Samples were diluted in 50% acetonitrile/0.1% trifluoroacetic acid. Equal volumes of sample and a saturated solution of α-cyano-4–hydroxycinnamic acid in 50% acetonitrile/0.1% trifluoroacetic acid, were mixed on the MALDI target plate and allowed to dry in air. Mass spectra were acquired using a Bruker Daltonics UltraFlex II MALDI-TOF/TOF mass spectrometer. The mass range 500–6000 Da was scanned in Reflectron and Linear modes using a range of laser powers to achieve the best resolution. The spectra were calibrated using an external calibration of known mass standards.

Zeta–average quantification

LL-37 (50 μg/ml) was incubated with carbon black nanoparticles at the concentrations indicated in various diluents for 1 and 4 h at 37˚C. The diluent used was DMEM supplemented with 1% Ultroser G. The samples were all vortexed before being transferred to a disposable cuvette and the

Z-average was obtained using a Zetasizer NanoZS (Malvern Instruments, Worcestershire, U.K.). The protocol was carried out in accordance with the manufacturer's instructions and the readings were measured as follows: eight runs each lasting 10 s were taken and a mean calculated by the software. A quality report was produced for each sample.

The impact of nanoparticle exposure on the antiviral activity of LL-37

LL-37 and carbon nanoparticles were incubated together for 1 h at room temperature prior to exposure to rhinovirus for an additional 1 h before inoculation of the 96-well plates. The physiologically relevant concentration of LL-37 (75 μg/ml) was used as it was shown to have a significant effect on reducing viral titer. WI-38 cells were seeded into a 96-well plate (5000 cells per well) with complete culture media. The plate was incubated overnight at 37˚C, 5% CO_2 prior to infection. The tissue culture infectious dose, where 50% of a cell culture exhibits pathological change following inoculation, was used as the measure of viral infectivity. To determine the tissue culture infectious dose, serial dilutions of the virus were prepared (1:10) i.e., 100 μl of the propagated RV1B virus was diluted in 900 μl of infection media. The viral titer was determined by addition of each dilution (200 μl) to each well containing cells. Plates were then incubated for ∼2 h at 33˚C, 5% CO_2. The medium in each well was aspirated and was replaced with maintenance media and the plate was incubated at 33˚C, 5% CO_2 for 4–6 d to allow for viral replication. Plates were observed daily until the first observation of cytopathic effects and the viral titer recorded for each sample.

The impact of nanoparticle exposure on the antibacterial activity of LL-37

LB crystals (2 g) were dissolved in 100 ml of dH_2O and a single bacterial colony from the culture plates was added to 10 ml of sterile LB broth. This tube was incubated on a shaking platform at 37˚C overnight. The overnight bacterial solution was diluted in fresh LB broth (1:10 dilution) and incubated at 37˚C for a further 2 h. The OD of the bacterial suspension was then corrected to $0.1OD_{600}$ by dilution with serum-free culture medium (high-glucose DMEM). LB agar plates were made using the manufacturer's guidelines. The Miles and Misra method for estimating CFU per milliliter was used and the plates were incubated at 37˚C. Samples were prepared with LL-37 (75 μg/ml) and carbon black nanoparticles (50 μg/ml) and were preincubated for 1 h at 37˚C prior to exposure of samples to the bacteria for 4 h ($n = 6$).

The impact of nanoparticle exposure on the anti-biofilm activity of LL-37

P. aeruginosa (strain PA01) was cultured in LB broth overnight at 37˚C in 5% CO_2 as previously described (15). The overnight bacterial cultures were diluted to an OD of 0.1 OD_{600}, and 200 μl of the diluted culture was added to the desired number of wells on a 96-well plate and incubated for 24 h at 37˚C. After 24 h, each well was washed three times with 200 μl of PBS, before adding 200 μl of ethanol and incubating for 1 min to remove any unbound bacteria and PBS. Ethanol was removed and plates were left to dry in a fume cabinet without the lid for 10 min. Following the drying step, 1% crystal violet solution (200 μl) was added to each well and incubated for 2 min at room temperature. The crystal violet solution was then removed and the wells washed three times with PBS (200 μl) as before. The plate was left overnight to dry in the fume cabinet with the plate lid on. The following day the crystal violet was released into the wells by addition of 100% ethanol (200 μl). The dye was allowed to solubilize by covering the plates and incubating at room temperature for 10–15 min. The dye samples were then pipetted into a fresh plate and the OD was measured using a plate reader (LT5000; Labtech, East Sussex, U.K.) at 595 nm. A biofilm phenotype was defined as $OD_{595} \geq 0.17$; a weak biofilm formation was classified as OD_{595} between 0.17 and 1.0; and a strong biofilm was defined as $OD_{595} \geq 1.0$ (19).

LL-37 (20 μg/ml) was added to diluted bacterial cultures prior to addition to the 96-well plates. Lower concentrations of peptide were used in comparison with the bacterial and viral studies, as previously published studies show that bacterial biofilms were sensitive to the action of LL-37 at concentrations >0.5 μg/ml (20–22). Similarly, carbon nanoparticles were also added to diluted overnight bacterial cultures prior to their addition to the 96-well plates. Samples that contained both LL-37 and carbon nanoparticles were preincubated together for 1 h prior to addition to the diluted bacterial culture.

The impact of nanoparticle exposure on the LPS-neutralizing activity of LL-37

Type II lung epithelial cells (A549) were seeded in 96-well plates at 1×10^5 cells per well. Cells were cultured in DMEM (high glucose) supplemented with 1% penicillin streptomycin, 1% L-glutamine, and 10% FCS. LPS from *E. coli* 0111:B4 (100 ng/ml) (Sigma-Aldrich), LL-37 (25 μg/ml), and carbon black (50 μg/ml) were used. Previous studies have shown that LL-37 possessed LPS/endotoxin neutralization activity at concentrations >10 μg/ml (23, 24). The samples were preincubated for 1 h prior to exposure to the cells, and then incubated for 24 h before the supernatants were collected, and stored in 100 μl aliquots at −80˚C until required. For each ELISA, the samples were all analyzed on one plate.

A TNF-α (sensitivity 2 pg/ml) ELISA kit (ELISA MAX Deluxe set; BioLegend, London, U.K.) was performed according to the manufacturer's instructions using the frozen samples. Prior to use the samples were centrifuged at 13,000 × *g* for 10 min using a Hettich Universal 320R centrifuge (DJB Labcare) to remove unbound particles. Following the ELISA procedure, the absorbance was measured at 450 nm using a plate reader within 30 min.

Data analysis

The results are expressed as mean ± SEM. All statistical analysis was conducted using either one- or two-way ANOVA using GraphPad Prism 6.0 as appropriate to determine statistical significance. A p value ≤0.05 was regarded as statistically significant.

Results

Assessment of peptide-nanoparticle interactions

An LL-37–specific ELISA was used to detect measurable concentrations of LL-37 following exposure to carbon black nanoparticles (Fig. 1). It was found that there was a significant decrease in the concentrations of detectable LL-37 with all concentrations of carbon black nanoparticles tested (25, 50, and 100 μg/ml), with samples containing both LL-37 and carbon nanoparticles measured at similar protein concentrations to those of the nanoparticle-only controls.

To investigate interactions occurring between LL-37 and carbon black nanomaterials resulting in structural alteration of the peptide, MALDI-TOF mass spectrometry was used to compare spectra between LL-37 only, and LL-37 exposed to carbon black nanoparticles (Fig. 2). This allowed detection of nanoparticle-mediated peptide cleavage or peptide degradation represented by more peaks in the spectra obtained. It was observed that the spectra obtained from the peptide-only analysis (Fig. 2A) was similar to that of the peptide treated with nanoparticles (Fig. 2B), indicating

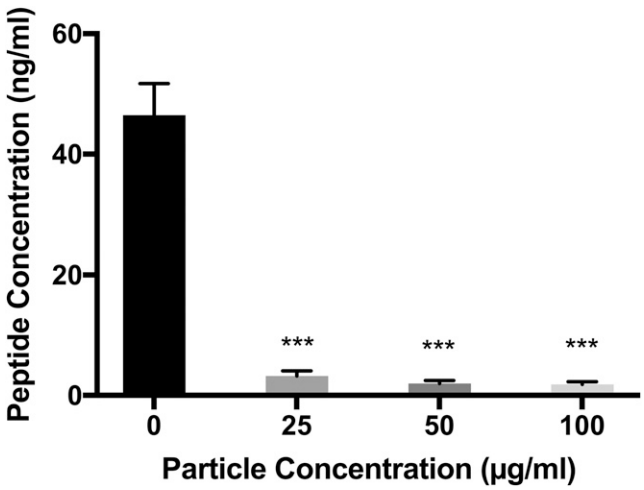

FIGURE 1. Carbon nanoparticle exposure alters Ab-mediated detection of LL-37. LL-37 (50 μg/ml) was incubated with carbon nanoparticles (0, 25, 50, and 100 μg/ml) for 4 h at 37˚C prior to detection of LL-37 peptide by commercial ELISA. Data represent the mean peptide concentrations (nanograms per milliliter) detected ± SEM for $n = 3$ independent experiments for each condition. One-way ANOVAs were performed to evaluate significance comparing the nanoparticle and peptide treatments to the LL-37–only control (***$p \leq 0.001$).

that LL-37 was neither cleaved nor degraded into smaller fragments in the presence of carbon nanoparticles.

We subsequently investigated the capacity for nanomaterials to inhibit the cross-linking potential of the LL-37 peptide (Fig. 3A). EGS was used as an amine cross-linking agent to promote the cross-linking of the peptide at primary amine sites located at the N terminus of the peptide, together with the amine groups on the side chains of lysine residues. LL-37 was shown to cross-link using EGS as evidenced by multiple bands visualized on an SDS-PAGE gel with a larger m.w. than that of the native peptide (Lane 4). LL-37–only samples resolved only one band with a molecular mass of ∼4 kDa (Lane 5). Resolution of LL-37 peptide treated with carbon nanoparticles prior to EGS (Lane 10) indicated that cross-linking was partially inhibited by pre-exposure to nanomaterials with the loss of two higher m.w. bands observed in Lane 4 reduced or missing (Lane 10).

To further characterize the physical properties of carbon nanoparticles following interaction with LL-37, the Z-average (hydrodynamic diameter) of the nanoparticles was measured using dynamic light scattering (DLS) over a 4 h period (Fig. 3B). DLS is frequently used to measure the size of particles within a given sample, and in this context, our aim was to measure nanoparticles before and after exposure to peptide to quantify the extent to which peptides were adsorbed to the surface of the nanoparticle, altering the physical characteristics. All treatments were incubated at 37˚C for 4 h and measured at intervals of 0, 1, and 4 h to determine if the duration of incubation impacted upon measurement of Z-average. It was determined that there was a significant increase in Z-average at all timepoints between control samples (nanoparticle only) and samples containing both nanomaterials and peptide. This observation was consistent at all timepoints tested, with larger Z-average values obtained at 4 h compared with the earlier timepoints.

Assessment of the antibacterial and antiviral capacity of LL-37 following carbon nanoparticle exposure

We assessed the impact of carbon nanoparticle exposure on the antiviral activity of LL-37 using a model minor-group rhinovirus strain (RV1B). LL-37 (75 μg/ml) treatment of virus induced a significant reduction in the detectable viral titer. However, LL-37 exposed to carbon black nanoparticles prior to treatment of RV1B failed to induce any significant reduction in measured viral titer compared with the virus-only control (Fig. 4A). Interestingly, although nanoparticles were observed to exhibit direct antiviral activity, this effect was also reduced by the interaction of the peptide and the nanoparticles.

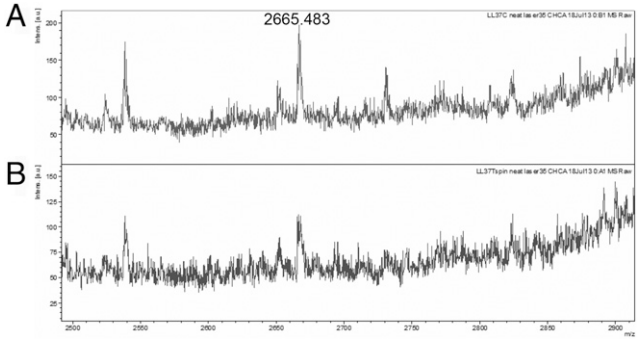

FIGURE 2. Exposure to carbon nanoparticles does not cause detectable fragmentation of LL-37 peptide in vitro. LL-37 (125 μg/ml) was subjected to MALDI-TOF mass spectrometry (reflectron mode) following exposure to carbon black nanoparticles (100 μg/ml) for 4 h at 37˚C. Data are represented as spectra and labeled mass values of LL-37 in the absence (**A**) and presence (**B**) of carbon nanoparticles.

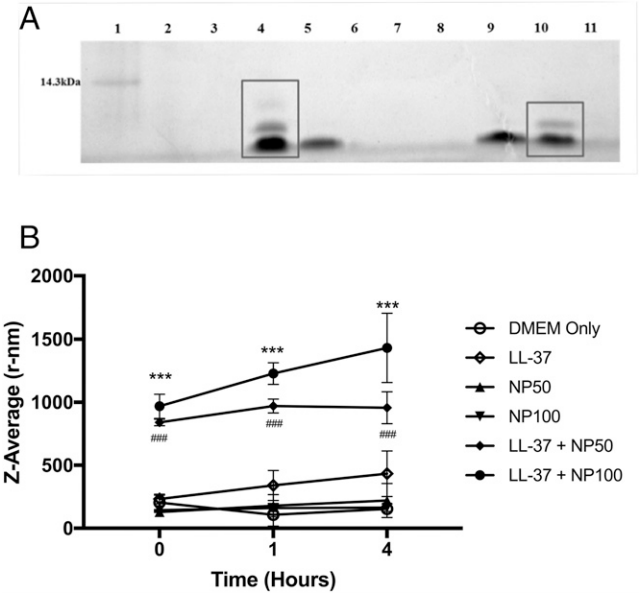

FIGURE 3. LL-37 interacts with carbon nanoparticles and alters cross-linking potential and nanoparticle size. (**A**) LL-37 (125 μg/ml) was pre-incubated with carbon black nanoparticles (100 μg/ml) for 1 h prior to the addition of EGS. The samples were then left for a further 30 min at 37˚C to allow the cross-linking to occur. Key: 1) protein marker, 2) empty, 3) EGS (2 mM) + dH_2O, 4) LL-37 + EGS (2 mM) + dH_2O, 5) LL-37 + dH_2O, 6) CB nano + dH_2O, 7) empty, 8) CB nano + EGS (2 mM) + dH_2O, 9) LL-37 + CB nano + dH_2O, 10) LL-37 + CB nano +EGS (2 mM) + dH_2O, and 11) dH_2O. (**B**) Carbon nanoparticles (100 μg/ml) were incubated in the presence and absence of LL-37 (50 μg/ml) for 4 h at 37˚C and particle size was assessed at 0, 1, and 4 h by DLS. The timepoint of 0 h represents T-0 following 10 min of sonication to ensure particle dispersal. Data are expressed as Zeta-average (Z-average) quantification (r-nm). A two-way ANOVA, with Bonferroni multiple comparisons test, was performed to evaluate significance comparing treatments to their respective controls ($^{***}p \leq 0.001$, $^{\#\#\#}p \leq 0.001$).

We further assessed impact of carbon nanoparticle exposure on the antibacterial activity of LL-37 against isolates of *S. aureus* and *E. coli*. Consistent with the findings of previous studies, LL-37 displayed significant antimicrobial activity against both *S. aureus* and *E. coli* (Fig. 4B, 4C, respectively) (25, 26). In agreement with the impact of nanoparticle exposure on the antiviral activity of the peptide, LL-37 showed a reduction in antibacterial activity when preincubated with the nanoparticles. Nanoparticle exposure alone had no significant effect on the bacterial populations.

We assessed whether carbon nanoparticles could inhibit the anti-biofilm–forming activity of LL-37 (Fig. 5). When assessing the effect of LL-37 against the biofilm-forming ability of *P. aeruginosa* (PAO1), we found a significant reduction in biofilm formation compared with control, as indicated by a reduction in biofilm absorbance in the presence of LL-37 (20 μg/ml), which was consistent with previous studies (21). We observed that there was no significant reduction in the absorbance measured in the presence of carbon nanoparticle alone, indicating that the nanoparticles used did not have any inhibitory effects on the biofilm-forming ability of *P. aeruginosa*. It was also observed that LL-37 did not lose its ability to inhibit biofilm formation as a result of carbon nanoparticle exposure, suggesting that the anti-biofilm–formation function of LL-37 is not detrimentally affected by the presence of carbon nanoparticles.

Finally, the potential for nanoparticles to alter LL-37–mediated inhibition of LPS signaling was assessed in a lung epithelial cell model. When exposed to LPS, the A549 lung type II epithelial cell

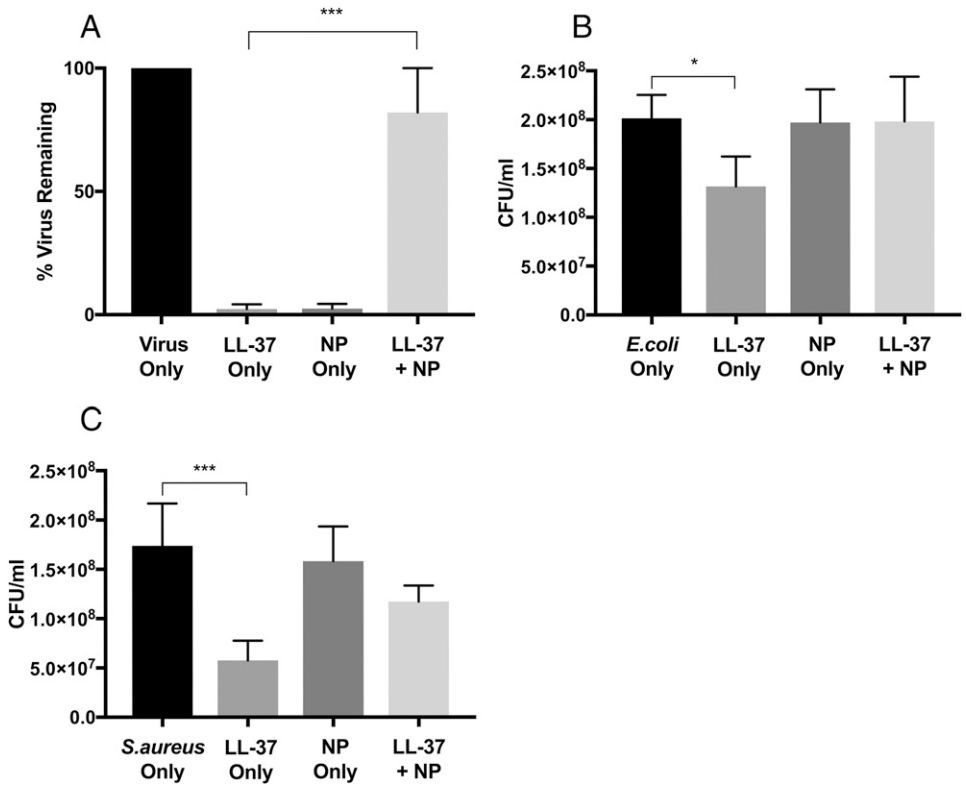

FIGURE 4. Carbon nanoparticle exposure inhibits the direct antiviral and antibacterial activity of LL-37. (**A**) LL-37 (75 μg/ml) was incubated with carbon black nanoparticles (100 μg/ml) for 1 h prior to exposure to rhinovirus (RV1B) for 1 h. Data represent the percentage of virus remaining following incubation with peptide only, nanoparticles only, or peptide + nanoparticles ($n = 5$). A one-way ANOVA was performed to evaluate statistical significance, with Bonferroni multiple comparisons test used to compare samples to the control (***$p \leq 0.001$). (**B** and **C**) LL-37 (75 μg/ml) was incubated with carbon black nanoparticles (100 μg/ml) for 1 h prior to exposure to (B) *S. aureus* (NCIB 6571; Oxford Strain) or (C) *E. coli* (NCIB 86 strain) for 1 h. Data represent the CFU remaining following incubation with peptide only, nanoparticles only, or peptide + nanoparticles ($n = 5$). A one-way ANOVA was performed to evaluate statistical significance, with Bonferroni multiple comparisons test used to compare samples to the control (*$p < 0.05$, ***$p \leq 0.001$).

line was shown to significantly increase the release of the proinflammatory cytokine TNF-α (Fig. 6). This effect was reduced by the addition of LL-37 but not the scrambled LL-37 control peptide, as expected. However, when LL-37 was incubated with carbon nanoparticles prior to assessing inhibition of LPS signaling, it was determined that there was no decrease in the concentrations of TNF-α produced as a result of LPS stimulation. As a control, carbon nanoparticle–only treatments were also conducted to control against conflicting proinflammatory signals masking the LL-37 dampening effect through a different signaling mechanism, but it was determined that carbon nanoparticles alone did not induce TNF-α release under these conditions.

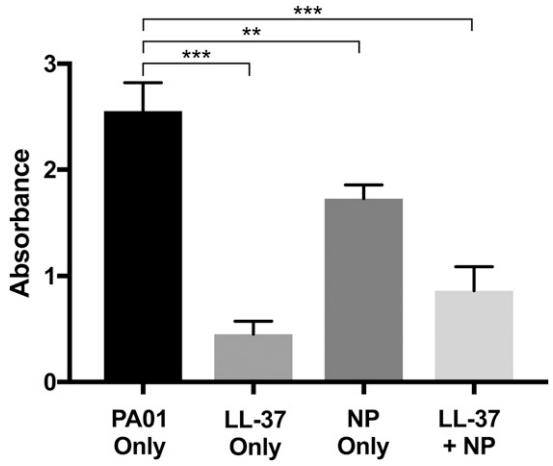

FIGURE 5. Carbon nanoparticle exposure does not inhibit the antibiofilm activity of LL-37 against *P. aeruginosa*. LL-37 and/or carbon black nanoparticles were incubated with log-phase *P. aeruginosa* (strain PA01) for 24 h and bacterial biofilm formation was assessed using 1% crystal violet solution. Data represent absorbance of biofilm at 450 nm from four independent experiments ($n = 4$). A one-way ANOVA was performed to evaluate statistical significance, with Dunnett multiple comparisons test used to compare treatments to the control (***$p \leq 0.001$, **$p \leq 0.01$).

Discussion

Nanoparticles are present at high concentrations in ambient air pollution and it is well documented that there are higher incidences of adverse respiratory episodes and infections in asthma patients in areas of high particulate air pollution (27, 28). However, the mechanism underlying this observation remains unclear. It has been documented in several studies that proteins or peptides interacting with nanoparticles can undergo structural changes, which in turn can cause a change, or loss, of function (29–31). The aim of this study was to investigate if nanomaterials alter the activity of HDPs, with the hypothesis that this could lead to increased susceptibility to infection in individuals who are exposed to consistently high concentrations of combustion-derived nanoparticles. The focus of this study was the sole human cathelicidin LL-37, a peptide that has been demonstrated to play key roles within the innate immune system due to its pluripotent roles in host defense.

We investigated whether carbon nanoparticles, as a model of combustion-derived particulate air pollution nanomaterials, could alter the structural properties of LL-37. We examined whether it

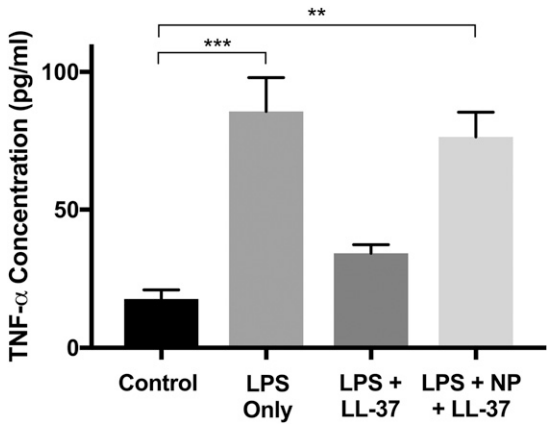

FIGURE 6. Carbon nanoparticle exposure inhibits the LPS neutralizing activity of LL-37 in vitro LL-37 peptide and carbon nanoparticles were preincubated for 1 h prior to the addition to A549 cells with simultaneous addition of LPS. Cells were incubated for 24 h at 37°C, 5% CO_2. Supernatants were collected and an ELISA was used to measure TNF-α release by cells in response to each of the samples. Data represent concentration of TNF-α measured from three independent experiments ($n = 3$). A one-way ANOVA was performed, with Bonferroni multiple comparisons tests, to evaluate statistical significance comparing all treatments to the control (***$p \leq 0.001$, **$p \leq 0.01$).

was possible for Ab binding to the LL-37 peptide to still occur following exposure to carbon nanoparticles. Using an LL-37–specific ELISA, we showed that following nanoparticle exposure, the LL-37 epitope was no longer identifiable or accessible, translating to a significant reduction in the concentrations of LL-37 detected. These data suggested there was an interaction occurring whereby the peptide epitope had become blocked or distorted. It has previously been shown that a wide range of proteins can bind to a variety of nanoparticles, including silver, carbon, and silicon, in a phenomenon characterized as a protein corona (18, 32). These proteins can include, but are not limited to, albumin, surfactant proteins A and D, and IgG (33–35). This is also consistent with recent studies that revealed that diesel exhaust nanoparticles have the capacity to bind to a wide range of proteins that are commonly found in bronchoalveolar lavage fluid, and that this process subsequently increased diesel exhaust particle and carbon nanoparticle uptake into the differentiated macrophage-like cell line THP-1 (36). However, characterization of any functional alteration of the proteins analyzed remains to be undertaken.

Of note, it has been suggested that the presence of ambient particulate matter and engineered nanoparticles can interfere with the detection of biologically significant peptides and proteins (37, 38), and thus we further used a number of approaches to characterize structural and functional alteration of the cathelicidin peptide. In this instance, we elected to use superphysiological concentrations of LL-37 (125 μg/ml) in our analysis to allow effective visualization of the impact of nanomaterial exposure. MALDI-TOF mass spectrometry analysis of LL-37 in the presence and absence of carbon nanoparticles determined that carbon nanoparticle exposure did not have an impact on the molecular mass of the peptide, suggesting it was still intact following exposure (cleavage or degradation of the peptide would be indicated by the presence of multiple smaller lower mass fragments in the spectra). Previous studies have revealed a role for bacterial proteinases in the degradation of LL-37 (39) but physical alteration of the peptide by inorganic material has thus far not been evidenced.

As an alternative approach to assess nanoparticle-mediated alteration of the peptide, we investigated the cross-linking ability of LL-37 utilizing EGS. EGS is an amine cross-linker and we hypothesized that it would induce conjugation at the amine end of the peptide, together with the amide group on the lysine residues. Accordingly, we estimated up to seven potential cross-linking sites on LL-37 were available, all of which were situated between amino acid residues 8–25, separated by only a few other amino acids. In this context, peptide conjugation would be represented by multiple heavier m.w. bands on an SDS-PAGE gel, but inhibition by nanoparticle exposure would reduce additional band formation. We found that LL-37, in the absence of nanoparticles, did cross-link in the presence of EGS, as demonstrated by the presence of multiple bands at a higher m.w. (Fig. 3). However, our data suggested carbon nanoparticle exposure resulted in only a partial inhibition of the LL-37 conjugation. Although our data indicated cross-linking of LL-37 was only affected to a minor extent by carbon nanoparticles, the secondary structure of the peptide may have been changed by nanomaterial exposure, although not necessarily at these particular sites.

To directly assess the potential for the LL-37 peptide to bind to the surface of the carbon nanoparticles, we assessed the aerodynamic diameter of the particles in the presence and absence of peptide to determine if particle size was altered. In treatments that contained peptide, nanoparticles had significantly larger Z-average values, corresponding to a larger diameter in comparison with control samples (i.e., cell medium, LL-37, or nanoparticles by themselves). The increase in the diameter of the particles occurred at an early time point, demonstrating that the binding process was occurring very rapidly between peptide and nanoparticle. These data could suggest that 1) the particles are exhibiting increased aggregation in the presence of the peptide, or 2) the particles are adsorbing the peptide to their surface, resulting in a physically larger particle. Although it is feasible that aggregation of nanoparticles could result in the measurement of larger particle sizes, when considered in the context of our other data, there is sufficient evidence to hypothesize that peptides are, at least partially, being adsorbed to the particle surface. This is in the context of the detection of the peptide using protein analysis methods such as ELISA, suggesting a loss of physically detectable peptide, although this can be problematic as considered above. Whereas other studies using mixed protein fluids such as plasma have suggested proteins involved in complement activation and coagulation (40) predominantly among the major components of a protein corona, our data suggest that peptides involved in host defense may also be a key part of this composition.

To assess the impact of nanomaterial exposure on peptide function, we modeled the antimicrobial functions of LL-37 against two bacterial species, *S. aureus* and *E. coli*, as well as rhinovirus RV1B. To model the lung environment the treatments were all conducted in serum-free media, because serum and plasma proteins would not normally be present in the lung unless there was structural damage to the respiratory vasculature. The species chosen for this study were all clinically relevant pathogens, implicated in contributing to the pathogenesis of conditions such as ventilator associated pneumonia, cystic fibrosis, and neonatal pneumonia (41, 42). The concentration of LL-37 used in this assessment (75 μg/ml) was superphysiological in the context of prior concentration estimates in healthy and inflamed lungs (43, 44), but represented a consistent antimicrobial level of this peptide across all pathogens tested.

Consistent with previously published studies (19, 25), LL-37 was shown to have direct antibacterial activity against *S. aureus* and *E. coli*. However, the potent antibacterial activity of LL-37 was lost following the addition of carbon black nanoparticles. We recently demonstrated a significant role for cathelicidins in the innate response to influenza virus (45) and rhinovirus 1B (46), and these data suggest that the antiviral activity of LL-37 was also reduced by exposure to nanomaterials.

We also investigated the impact of nanomaterial exposure on the anti-biofilm activity of LL-37, as this peptide has previously been shown to have the capacity to disrupt biofilm formation (20–22). To assess whether LL-37 was able to retain its anti-biofilm activity, a well-established biofilm formation assay was used with *P. aeruginosa* as the model organism. We showed that LL-37 was effective against *P. aeruginosa* biofilm formation as expected, and that this activity was generally preserved with exposure to nanoparticles. However, the anti-biofilm activity of the nanoparticles themselves may have influenced this finding as there was a moderate drop in biofilm formation observed when treatment consisted of nanoparticles in the absence of peptide. Previous studies have noted that silver nanoparticles have antimicrobial activity against *P. aeruginosa* (47), but the antimicrobial activity of carbon nanoparticles against *P. aeruginosa* is not yet fully established.

Finally we investigated the potential for nanomaterials to inhibit the LPS and endotoxin neutralization ability of LL-37, an important property of the peptide that could contribute significantly to the host inflammatory response together with enhancing pathogen clearance (23, 24). LPS predominantly signals through TLR 4 and activates the production and release of inflammatory cytokines such as TNF-α. In A549 cells treated with LPS, a robust TNF-α response was measured and, as expected, cytokine production was effectively decreased in the presence of LL-37 (25 μg/ml) due to the well-documented LPS neutralization ability of the peptide. However, our data also indicated that LL-37 lost the capacity to reduce LPS-mediated proinflammatory signaling in the presence of carbon nanoparticles. Although this is a powerful indication of the potential impact of nanoparticle exposure on the ability of a host cell to respond to infection, further studies are required to fully characterize the mechanism of action in this instance.

The data presented in this study suggest strongly that nanomaterials are capable of inhibiting normal cathelicidin activity. Although the focus of this study is the loss of peptide function following nanoparticle exposure, we also believe our study indicates that there is a role for HDP in the formation of the protein corona. However, although other groups have shown that the rapid formation of protein coronas around nanoparticles can affect their pathobiological effects (via reduction of thrombocyte activation, or reduction in hemolysis), it is as yet unclear whether this impairment can occur in the presence of small molecules such as HDP. However, in the context of this study, masking the potential toxicity of the nanomaterials may be a consequence of this.

In summary, we have shown that carbon nanoparticles interact with LL-37, a process that involves a structural change in the LL-37 peptide. We suggest that this structural change is mediated through alteration of the α helical structure of the peptide rather than by direct cleavage or degradation. We further suggest that a loss of HDP activity as a result of nanomaterial exposure could result in an increased susceptibility to infection. This could have significant consequences for immunocompromised individuals and further studies are required to assess the impact of engineered and combustion-derived nanomaterials on other key host defense molecules, particularly in cases where individuals are repeatedly exposed to unsafe concentrations of environmental particulate air pollution.

Acknowledgments

We thank Dr. Gary Hutchison for expert advice.

Disclosures

The authors have no financial conflicts of interest.

References

1. BéruBé, K., D. Balharry, K. Sexton, L. Koshy, and T. Jones. 2007. Combustion-derived nanoparticles: mechanisms of pulmonary toxicity. *Clin. Exp. Pharmacol. Physiol.* 34: 1044–1050.
2. Bonner, J. C. 2010. Nanoparticles as a potential cause of pleural and interstitial lung disease. *Proc. Am. Thorac. Soc.* 7: 138–141.
3. Jakab, G. J. 1993. The toxicologic interactions resulting from inhalation of carbon black and acrolein on pulmonary antibacterial and antiviral defenses. *Toxicol. Appl. Pharmacol.* 121: 167–175.
4. Sigaud, S., C. A. Goldsmith, H. Zhou, Z. Yang, A. Fedulov, A. Imrich, and L. Kobzik. 2007. Air pollution particles diminish bacterial clearance in the primed lungs of mice. *Toxicol. Appl. Pharmacol.* 223: 1–9.
5. Bowdish, D. M., D. J. Davidson, M. G. Scott, and R. E. Hancock. 2005. Immunomodulatory activities of small host defense peptides. *Antimicrob. Agents Chemother.* 49: 1727–1732.
6. Barlow, P. G., E. G. Findlay, S. M. Currie, and D. J. Davidson. 2014. Antiviral potential of cathelicidins. *Future Microbiol.* 9: 55–73.
7. Findlay, F., L. Proudfoot, C. Stevens, and P. G. Barlow. 2016. Cationic host defense peptides; novel antimicrobial therapeutics against Category A pathogens and emerging infections. *Pathog. Glob. Health* 110: 137–147.
8. Xhindoli, D., S. Pacor, M. Benincasa, M. Scocchi, R. Gennaro, and A. Tossi. 2016. The human cathelicidin LL-37–A pore-forming antibacterial peptide and host-cell modulator. *Biochim. Biophys. Acta* 1858: 546–566.
9. Sørensen, O. E., P. Follin, A. H. Johnsen, J. Calafat, G. S. Tjabringa, P. S. Hiemstra, and N. Borregaard. 2001. Human cathelicidin, hCAP-18, is processed to the antimicrobial peptide LL-37 by extracellular cleavage with proteinase 3. *Blood* 97: 3951–3959.
10. Agerberth, B., J. Charo, J. Werr, B. Olsson, F. Idali, L. Lindbom, R. Kiessling, H. Jörnvall, H. Wigzell, and G. H. Gudmundsson. 2000. The human antimicrobial and chemotactic peptides LL-37 and alpha-defensins are expressed by specific lymphocyte and monocyte populations. *Blood* 96: 3086–3093.
11. Coyle, C., N. Wheelhouse, M. Jacques, D. Longbottom, P. Svoboda, J. Pohl, W. C. Duncan, M. T. Rae, and P. G. Barlow. 2016. Ovine trophoblasts express cathelicidin host defence peptide in response to infection. *J. Reprod. Immunol.* 117: 10–16.
12. De Yang, Chen, A. P. Schmidt, G. M. Anderson, J. M. Wang, J. Wooters, J. J. Oppenheim,and O. Chertov. 2000. LL-37, the neutrophil granule- and epithelial cell-derived cathelicidin, utilizes formyl peptide receptor-like 1 (FPRL1) as a receptor to chemoattract human peripheral blood neutrophils, monocytes, and T cells. *J. Exp. Med.* 192: 1069–1074.
13. Koczulla, R., G. von Degenfeld, C. Kupatt, F. Krötz, S. Zahler, T. Gloe, K. Issbrücker, P. Unterberger, M. Zaiou, C. Lebherz, et al. 2003. An angiogenic role for the human peptide antibiotic LL-37/hCAP-18. *J. Clin. Invest.* 111: 1665–1672.
14. Davidson, D. J., A. J. Currie, G. S. Reid, D. M. Bowdish, K. L. MacDonald, R. C. Ma, R. E. Hancock, and D. P. Speert. 2004. The cationic antimicrobial peptide LL-37 modulates dendritic cell differentiation and dendritic cell-induced T cell polarization. *J. Immunol.* 172: 1146–1156.
15. Barlow, P. G., P. E. Beaumont, C. Cosseau, A. Mackellar, T. S. Wilkinson, R. E. Hancock, C. Haslett, J. R. Govan, A. J. Simpson, and D. J. Davidson. 2010. The human cathelicidin LL-37 preferentially promotes apoptosis of infected airway epithelium. *Am. J. Respir. Cell Mol. Biol.* 43: 692–702.
16. Barlow, P. G., Y. Li, T. S. Wilkinson, D. M. Bowdish, Y. E. Lau, C. Cosseau, C. Haslett, A. J. Simpson, R. E. Hancock, and D. J. Davidson. 2006. The human cationic host defense peptide LL-37 mediates contrasting effects on apoptotic pathways in different primary cells of the innate immune system. *J. Leukoc. Biol.* 80: 509–520.
17. Lacerda, S. H., J. J. Park, C. Meuse, D. Pristinski, M. L. Becker, A. Karim, and J. F. Douglas. 2010. Interaction of gold nanoparticles with common human blood proteins. *ACS Nano* 4: 365–379.
18. Cedervall, T., I. Lynch, M. Foy, T. Berggård, S. C. Donnelly, G. Cagney, S. Linse, and K. A. Dawson. 2007. Detailed identification of plasma proteins adsorbed on copolymer nanoparticles. *Angew. Chem. Int. Ed. Engl.* 46: 5754–5756.
19. Clinical and Laboratory Standards Institute. 2012. *Methods for Dilution Antimicrobial Susceptibility Tests for Bacteria That Grow Aerobically* (CLSI document M07-A9), Approved Standard—9th Ed. Clinical and Laboratory Standards Institute, Wayne, PA.
20. Dean, S. N., B. M. Bishop, and M. L. van Hoek. 2011. Natural and synthetic cathelicidin peptides with anti-microbial and anti-biofilm activity against *Staphylococcus aureus*. *BMC Microbiol.* 11: 114.
21. Nagant, C., B. Pitts, K. Nazmi, M. Vandenbranden, J. G. Bolscher, P. S. Stewart, and J. P. Dehaye. 2012. Identification of peptides derived from the human antimicrobial peptide LL-37 active against biofilms formed by *Pseudomonas aeruginosa* using a library of truncated fragments. *Antimicrob. Agents Chemother.* 56: 5698–5708.
22. Overhage, J., A. Campisano, M. Bains, E. C. Torfs, B. H. Rehm, and R. E. Hancock. 2008. Human host defense peptide LL-37 prevents bacterial biofilm formation. *Infect. Immun.* 76: 4176–4182.
23. Ciornei, C. D., T. Sigurdardóttir, A. Schmidtchen, and M. Bodelsson. 2005. Antimicrobial and chemoattractant activity, lipopolysaccharide neutralization, cytotoxicity, and inhibition by serum of analogs of human cathelicidin LL-37. *Antimicrob. Agents Chemother.* 49: 2845–2850.
24. Rosenfeld, Y., N. Papo, and Y. Shai. 2006. Endotoxin (lipopolysaccharide) neutralization by innate immunity host-defense peptides. Peptide properties and plausible modes of action. *J. Biol. Chem.* 281: 1636–1643.
25. Pompilio, A., M. Scocchi, S. Pomponio, F. Guida, A. Di Primio, E. Fiscarelli, R. Gennaro, and G. Di Bonaventura. 2011. Antibacterial and anti-biofilm effects of cathelicidin peptides against pathogens isolated from cystic fibrosis patients. *Peptides* 32: 1807–1814.

26. Turner, J., Y. Cho, N. N. Dinh, A. J. Waring, and R. I. Lehrer. 1998. Activities of LL-37, a cathelin-associated antimicrobial peptide of human neutrophils. *Antimicrob. Agents Chemother.* 42: 2206–2214.
27. Guarnieri, M., and J. R. Balmes. 2014. Outdoor air pollution and asthma. *Lancet* 383: 1581–1592.
28. Habre, R., E. Moshier, W. Castro, A. Nath, A. Grunin, A. Rohr, J. Godbold, N. Schachter, M. Kattan, B. Coull, and P. Koutrakis. 2014. The effects of PM2.5 and its components from indoor and outdoor sources on cough and wheeze symptoms in asthmatic children. *J. Expo. Sci. Environ. Epidemiol.* 24: 380–387.
29. Koutsopoulos, S., K. Patzsch, W. T. Bosker, and W. Norde. 2007. Adsorption of trypsin on hydrophilic and hydrophobic surfaces. *Langmuir* 23: 2000–2006.
30. Cukalevski, R., M. Lundqvist, C. Oslakovic, B. Dahlbäck, S. Linse, and T. Cedervall. 2011. Structural changes in apolipoproteins bound to nanoparticles. *Langmuir* 27: 14360–14369.
31. Lundqvist, M., I. Sethson, and B. H. Jonsson. 2004. Protein adsorption onto silica nanoparticles: conformational changes depend on the particles' curvature and the protein stability. *Langmuir* 20: 10639–10647.
32. Cedervall, T., I. Lynch, S. Lindman, T. Berggård, E. Thulin, H. Nilsson, K. A. Dawson, and S. Linse. 2007. Understanding the nanoparticle-protein corona using methods to quantify exchange rates and affinities of proteins for nanoparticles. *Proc. Natl. Acad. Sci. USA* 104: 2050–2055.
33. Zhang, S., H. Yang, X. Ji, and Q. Wang. 2016. Binding analysis of carbon nanoparticles to human immunoglobulin G: elucidation of the cytotoxicity of CNPs and perturbation of immunoglobulin conformations. *Spectrochim. Acta A Mol. Biomol. Spectrosc.* 154: 33–41.
34. Zhang, W., Q. Zhang, F. Wang, L. Yuan, Z. Xu, F. Jiang, and Y. Liu. 2015. Comparison of interactions between human serum albumin and silver nanoparticles of different sizes using spectroscopic methods. *Luminescence* 30: 397–404.
35. Mortimer, G. M., N. J. Butcher, A. W. Musumeci, Z. J. Deng, D. J. Martin, and R. F. Minchin. 2014. Cryptic epitopes of albumin determine mononuclear phagocyte system clearance of nanomaterials. *ACS Nano* 8: 3357–3366.
36. Shaw, C. A., G. M. Mortimer, Z. J. Deng, E. S. Carter, S. P. Connell, M. R. Miller, R. Duffin, D. E. Newby, P. W. Hadoke, and R. F. Minchin. 2016. Protein corona formation in bronchoalveolar fluid enhances diesel exhaust nanoparticle uptake and pro-inflammatory responses in macrophages. *Nanotoxicology* 10: 981–991.
37. Herseth, J. I., A. I. Totlandsdal, S. Bytingsvik, J. Kaur, M. Noer, and A. K. Bølling. 2013. The challenge of obtaining correct data for cellular release of inflammatory mediators after in vitro exposure to particulate matter. *Toxicol. Lett.* 221: 110–117.
38. Kroll, A., M. H. Pillukat, D. Hahn, and J. Schnekenburger. 2012. Interference of engineered nanoparticles with in vitro toxicity assays. *Arch. Toxicol.* 86: 1123–1136.
39. Schmidtchen, A., I. M. Frick, E. Andersson, H. Tapper, and L. Björck. 2002. Proteinases of common pathogenic bacteria degrade and inactivate the antibacterial peptide LL-37. *Mol. Microbiol.* 46: 157–168.
40. Lai, W., Q. Wang, L. Li, Z. Hu, J. Chen, and Q. Fang. 2017. Interaction of gold and silver nanoparticles with human plasma: analysis of protein corona reveals specific binding patterns. *Colloids Surf. B Biointerfaces* 152: 317–325.
41. Sievert, D. M., P. Ricks, J. R. Edwards, A. Schneider, J. Patel, A. Srinivasan, A. Kallen, B. Limbago, and S. Fridkin, National Healthcare Safety Network (NHSN) Team and Participating NHSN Facilities. 2013. Antimicrobial-resistant pathogens associated with healthcare-associated infections: summary of data reported to the National Healthcare Safety Network at the Centers for Disease Control and Prevention, 2009-2010. *Infect. Control Hosp. Epidemiol.* 34: 1–14.
42. Wang, H. J., H. Shi, W. Zhou, Z. Q. Hu, L. Y. Mu, M. Su, and Y. M. Jiang. 2012. Common pathogens and clinical characteristics of neonatal pneumonia. *Zhongguo Dang Dai Er Ke Za Zhi* 14: 898–902.
43. Chen, C. I., S. Schaller-Bals, K. P. Paul, U. Wahn, and R. Bals. 2004. Beta-defensins and LL-37 in bronchoalveolar lavage fluid of patients with cystic fibrosis. *J. Cyst. Fibros.* 3: 45–50.
44. Schaller-Bals, S., A. Schulze, and R. Bals. 2002. Increased levels of antimicrobial peptides in tracheal aspirates of newborn infants during infection. *Am. J. Respir. Crit. Care Med.* 165: 992–995.
45. Barlow, P. G., P. Svoboda, A. Mackellar, A. A. Nash, I. A. York, J. Pohl, D. J. Davidson, and R. O. Donis. 2011. Antiviral activity and increased host defense against influenza infection elicited by the human cathelicidin LL-37. *PLoS One* 6: e25333.
46. Sousa, F. H., V. Casanova, F. Findlay, C. Stevens, P. Svoboda, J. Pohl, L. Proudfoot, and P. G. Barlow. 2017. Cathelicidins display conserved direct antiviral activity towards rhinovirus. *Peptides* 95: 76–83.
47. Das, M. R., R. K. Sarma, R. Saikia, V. S. Kale, M. V. Shelke, and P. Sengupta. 2011. Synthesis of silver nanoparticles in an aqueous suspension of graphene oxide sheets and its antimicrobial activity. *Colloids Surf. B Biointerfaces* 83: 16–22.